GLUON DENSITY AND STRONG COUPLING FROM STRUCTURE FUNCTIONS AND MEASUREMENT OF F_L

VLADIMIR CHEKELIAN (SHEKELYAN)
Max-Planck-Institut für Physik
Werner-Heisenberg-Institut
Föhringer Ring 6, 80805 München, Germany
E-mail: shekeln@mppmu.mpg.de

In the first phase of data taking at the HERA *ep* collider various structure functions were measured. The precision of the measurements allows to make comprehensive analyses in the framework of QCD. Recent results on the gluon distribution function, the strong coupling constant $\alpha_s(M_Z^2)$ and the longitudinal structure function F_L are reviewed as well as studies of limits of applicability of the perturbative QCD approach.

1. Introduction

The study of the structure of hadrons has been a powerful means for establishing and testing of the theory of strong interactions and for the determination of the partonic structure of the nucleon. In Quantum Chromodynamics (QCD), structure functions are defined as a convolution of the universal parton momentum distributions inside the proton and coefficient functions, which contain information about the exchanged boson-parton interaction. At sufficiently large four-momentum transfer squared, Q^2, when the strong coupling α_s is small, a perturbative technique is applicable for QCD calculations of the coefficient and splitting functions. The latter represent the probability of a parton to emit another parton. Expressions for structure functions are determined by convolution integrals of appropriate sums over quarks of different flavours and the gluon, and they predict a logarithmic Q^2 dependence (evolution) of the structure functions. The perturbative QCD (pQCD) calculations are well established within the DGLAP [1] formalism to next-to-leading (NLO) order in the strong coupling and are close to completion to next-to-next-to-leading (NNLO) order [2].

Precision measurements of structure functions in a wide kinematic range allow comprehensive QCD analyses to determine the quark and gluon distributions inside the proton and the strong coupling constant $\alpha_s(M_Z^2)$. Such measurements allow also to explore pQCD application limits, for example at low x, where the parton density was found to rise steeply towards small x by the H1 and ZEUS experiments at HERA. Here, x is the fraction of proton momentum carried by the parton. In QCD this rise corresponds to an increase of the gluon density and is expected to slow down at highest energies (small x) due to gluon-gluon recombination, the so-called saturation effects.

Partons, i.e. quarks and gluons, enter differently into different structure functions. In deep inelastic scattering (DIS), the cross section of the neutral current (NC) process, mediated by a γ or Z^o-boson exchange, can be expressed in terms of three structure functions:

$$\frac{d^2\sigma^{e^\pm p->e^\pm X}}{dxdQ^2} = \frac{2\pi\alpha^2}{Q^4 x}\left[Y_+ F_2(x,Q^2) - y^2 F_L(x,Q^2) \mp Y_- xF_3(x,Q^2)\right], \tag{1}$$

where $y = Q^2/xs$ is the inelasticity, s is the center of mass energy squared, α is the fine structure constant and $Y_\pm = 1 \pm (1-y)^2$. The dominant contribution to the cross section is due to the proton structure function F_2, which is related in the framework of the quark-parton model (QPM) to the sum of the proton momentum fractions carried by the quarks and antiquarks in the proton weighted by the quark charges squared. The longitudinal structure function F_L, vanishing in the QPM, is directly sensitive to the gluon momentum distribution in the proton. The structure function xF_3 is related to valence quarks and is sizable only at large Q^2, with Q^2 comparable with the Z^o-boson mass squared.

In the first phase of data taking at the HERA ep collider (HERA I), the H1 and ZEUS experiments collected about 100 pb^{-1} of integrated luminosity each in the e^+p mode and about 15 pb^{-1} in the e^-p mode. These data provided information about structure functions, which are analysed in the framework of perturbative QCD. Further insight into the structure of the proton is obtained in semi-inclusive processes such as diffraction, heavy flavour and jet production, which are calculable in pQCD. This report concentrates on recent results on the gluon distribution function, the strong coupling constant $\alpha_s(M_Z^2)$ and checks for novel QCD effects.

2. QCD analyses of structure functions

The HERA I inclusive deep inelastic cross section measurements at low Q^2 and high Q^2 are reviewed in [3,4]. The determination of parton distribution functions (PDFs) in QCD analyses of these data, supplemented by data from fixed target experiments, are discussed in [4]. It is interesting to note that available measurements of the NC and CC (charged current) cross sections in $e^{\pm}p$ interactions at HERA allow PDF QCD fits [5,6], which lead to a quark flavour decomposition of parton densities based on HERA data only.

The improved quality of the recent QCD fits is achieved by more precise data and a new level of sophistication in the fitting techniques including a full treatment of correlated experimental systematic uncertainties. A new feature of the recent QCD analyses is also a pragmatic determination of PDF uncertainties and their physical predictions. One of the problems of the uncertainty estimation for fits with many data sets involved is related to a certain degree of inconsistency among them. Usually the one sigma error of a parameter in a fit is determined by variation of χ^2 by one unit from the minimum. However, the level of "inconsistency" should be reflected in the uncertainties. This can by achieved by the following modification of the above criterion: $\Delta\chi^2 = T^2$ [7,8,9], where T stands for a tolerance which is estimated from the level of (in)consistency of the data sets used in a particular QCD fit. For example, in the CTEQ6 fit the tolerance was taken to be 10 ($\Delta\chi^2 = 100$).

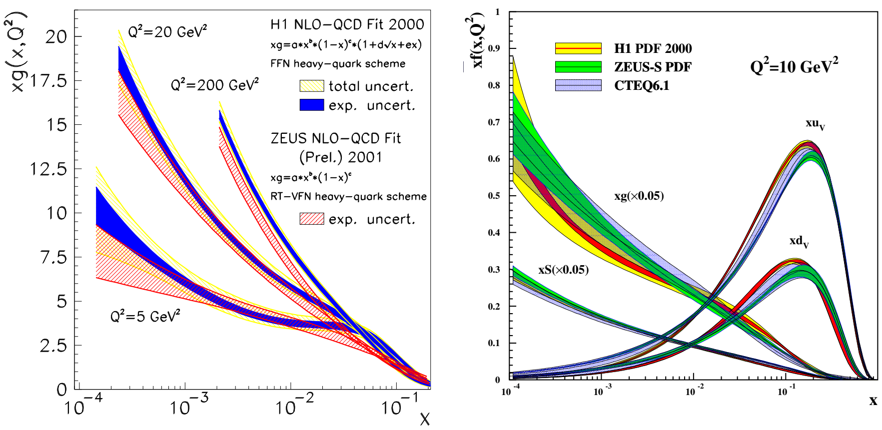

Figure 1. Gluon distributions for the dedicated xg&α_s fit of H1 and the ZEUS-S PDF fit for Q^2=5, 20, and 200 GeV^2 (left). Parton distributions for the H1 PDF 2000, ZEUS-S PDF and CTEQ6 fits for Q^2=10 GeV^2 (right). On the right plot the sea and gluon distributions are devided by a factor of 20.

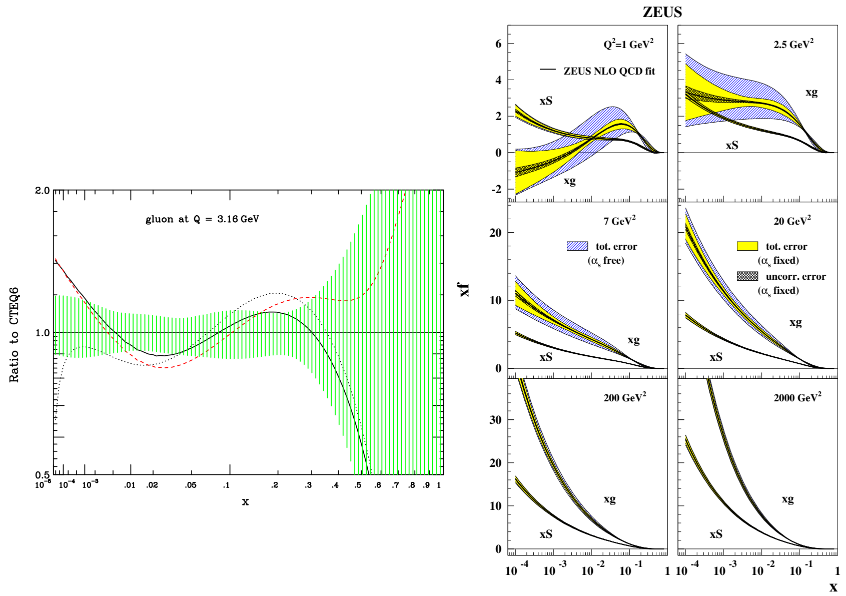

Figure 2. Relative gluon uncertainty as determined in the CTEQ6 fit (left). Gluon and sea distributions for the ZEUS-S PDF fit (right).

The H1 collaboration performed also a QCD fit [10] devoted especially to the determination of the gluon distribution and α_s (xg&α_s fit). A novel flavour decomposition of F_2 used in this fit allows to reduce the number of parton distributions to just two combinations (apart from the gluon density): "valence-like" and "sea-like". Thus, for this fit there is no need to include deuteron data in the fit, and the number of data sets can be reduced to a minimum: the H1 cross section data covering low x and the BCDMS μp data covering the region of large x (see also section 2.2).

2.1. *Gluon distribution*

The gluon distributions for different Q^2 from the dedicated xg&α_s fit [10] of H1, the H1 PDF 2000 [5] and the ZEUS-S PDF [6] fits are shown in Figure 1. The agreement of the different fits is reasonable, though there are clear differencies in the shape of the gluon distribution beyond the quoted error bands. The CTEQ6 fit, shown in Figure 1 (right), bridges the H1 and ZEUS results. The relative uncertainty band for the gluon distribution obtained in the CTEQ6 fit is about 10% at $x < 0.3$, Figure 2 (left).

The differences between the H1 and ZEUS fits have many sources. The

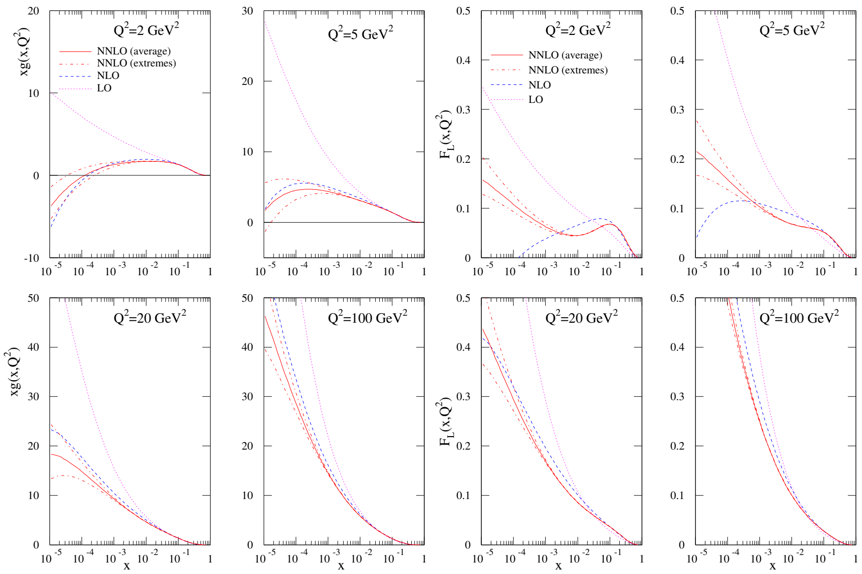

Figure 3. Gluon distributions (left) obtained from the LO, NLO and NNLO analyses of MRST and corresponding predictions for F_L (right) as a function of x for various values of Q^2.

assumptions and procedures are very different. This concerns for example the data sets used in the fits and the form of parameterisation of the parton densities at the starting scale for QCD evolution. Up to now there is no clear prescription how to take the last item properly into account in the uncertainty calculations. The HERA data themselves look very consistent, but it is not excluded that fits are sensitive to small features of the measurements.

The DGLAP evolution leads to a gluon distribution which rises towards small x at Q^2 above a few GeV^2, Figure 1. The gluon and sea distributions for the ZEUS-S PDF fit at different Q^2, including Q^2=1 GeV^2, are shown in Figure 2 (right). At the lowest Q^2 the rise of the sea density persists, while the gluon density flattens out at Q^2=2.5 GeV^2 and even becomes negative at Q^2=1 GeV^2. A simular feature is observed in the MRST NLO fit [8,11] shown in Figure 3 (left). While this is not necessarily a problem in itself, the gluon density from scaling violations is not an observable, it results in a distinct unphysical prediction for F_L shown in Figure 3 (right). Therefore, F_L measurements at HERA, discussed in section 3.3, are of a particular interest.

2.2. *Strong coupling constant* $\alpha_s(M_Z^2)$

Values for the strong coupling constant $\alpha_s(M_Z^2)$, determined in recent QCD analyses of DIS data, are summarised in Table 1. The results are rather consistent. However, the experimental uncertainties of $\alpha_s(M_Z^2)$ are very different due to different judgments on the $\Delta\chi^2$ criterion. The experimental errors are excellent (about 2%), if the canonical criterion $\Delta\chi^2 = 1$ is used in the fit.

The criterion $\Delta\chi^2 = 1$ can be applied only after careful consistency checks of the data sets used in the fit. For example in the dedicated $xg\&\alpha_s$ H1 fit only data from H1 and BCDMS μp are involved. Furthermore, for the BCDMS μp data a cut $y_\mu > 0.3$ is applied removing a region with large systematics uncertainties, where the deviations from the QCD fit (with full treatment of correlated systematics errors) exceed the systematic errors. Partial χ^2 of the H1 and BCDMS data points are shown as a function of $\alpha_s(M_Z^2)$ in Figure 4 (right). The χ^2 minima for both data sets are fully consistent and lie around $\alpha_s(M_Z^2) = 0.115$. The importance of the HERA data for the determination of α_s is illustrated in Figure 4 (left), where χ^2 for fits to “only H1” and “only BCDMS” data are shown. Without HERA data the gluon distribution from the fit to the BCDMS data becomes unrealistically flat at low x and drives $\alpha_s(M_Z^2)$ to about 0.110. The HERA data pin down the gluon density, and, as a result, $\alpha_s(M_Z^2)$ moves to 0.115 if both data sets are used in the fit.

Table 1. The strong coupling constant from NLO and NNLO QCD fits.

NLO QCD	$\Delta\chi^2$	$\alpha_s(M_Z^2)$
CTEQ6 [7]	100	$0.1165 \pm 0.0065(exp)$
ZEUS [6]	≈ 50	$0.1166 \pm 0.0008(uncor) \pm 0.0032(cor) \pm 0.0036(norm)$
		$\pm 0.0018(model) \pm 0.004(theory)$
MRST01 [8]	20	$0.1190 \pm 0.002(exp) \pm 0.003(theory)$
H1 [10]	1	$0.1150 \pm 0.0017(exp)^{+0.0009}_{-0.0005}(model) \pm 0.005(theory)$
Alekhin [12]	1	$0.1171 \pm 0.0015(exp) \pm 0.0033(theory)$
NNLO QCD	$\Delta\chi^2$	$\alpha_s(M_Z^2)$
Alekhin [12]	1	$0.1143 \pm 0.0014(exp) \pm 0.0013(theory)$

Most of the $\alpha_s(M_Z^2)$ determinations in Table 1 are performed in the NLO QCD approach. A limitation of the precision of $\alpha_s(M_Z^2)$ is due to the associated theoretical error calculated by varying the renormalisation and

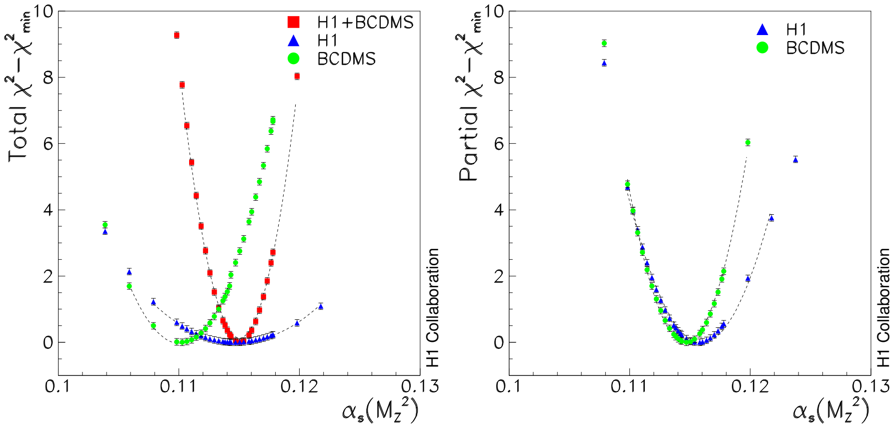

Figure 4. Total χ^2 in the $xg\&\alpha_s$ fits to H1 and BCDMS data separately and in the common fit to both data sets (left). Partial χ^2 contributions of the H1 and BCDMS data in the common fit (right).

factorisation scales. In the NNLO theory this uncertainty is reduced by a factor of 3, as one can see by comparing Alekhin's NNLO and NLO results, see also ref. [2].

3. The Low-x Regime

The region of low x accessed at HERA has been the subject of much debate (e.g. ref. [13]). The steep rise of F_2 discovered already in the first HERA measurements indicates a new partonic regime governed by a rising gluon density. This high parton density regime brings a possibility to reveal novel QCD effects related to e.g. unitarisation. The interpretation of experimental results in the lowest x domain should take into account the kinematical correlation between low x and low Q^2 at HERA. The latter domain brings its own complications related to the transition from the perturbative DIS regime to the photoproduction limit, where the perturbative approach is not working due to the large α_s and missing terms in theoretical calculations. The present experimental situation in inclusive measurements at low x obtained from detailed studies of derivatives of F_2 in $\ln x$ and $\ln Q^2$ and measurements of the longitudinal structure function F_L is discussed below.

3.1. *Rise of F_2 at low x*

In the double asymptotic limit, the DGLAP evolution equation can be solved and F_2 is expected to rise approximately as a power of x towards

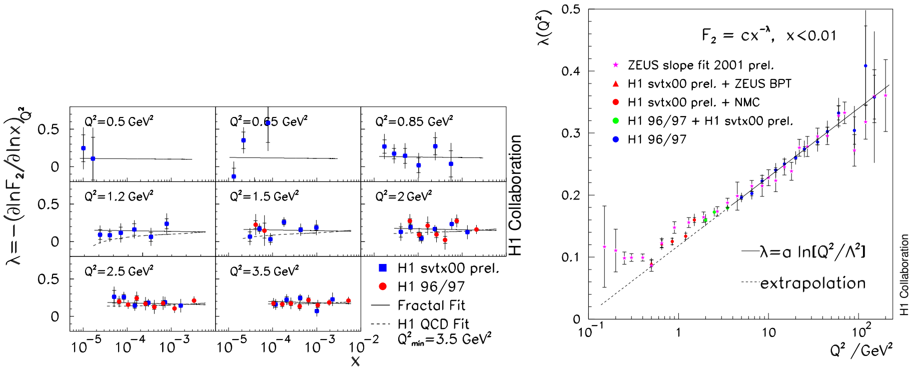

Figure 5. Local derivatives $\lambda = -(\partial \ln F_2(x,Q^2)/\partial \ln x)_{Q^2}$ (left) and fitted values of $\lambda(Q^2)$ (right).

low x. A power behaviour is also predicted in BFKL theory [14]. A damping of this rise would indicate the presence of novel QCD effects. A relevant observable for the investigation of the dynamics of this growth is the partial derivative of F_2 w.r.t. $\ln x$ at fixed Q^2

$$\lambda = -(\partial \ln F_2(x,Q^2)/\partial \ln x)_{Q^2} \ . \tag{2}$$

The high precision of the present F_2 data allowed H1 to measure this observable locally [15,16], as it is shown in Figure 5 (left) for the low Q^2 region. The measurements are consistent with no dependence of λ on x for $x < 0.01$. Thus, the monotonic rise of F_2 persists down to the lowest x measured at HERA, and no evidence for a change of this behaviour such as a damping of the growth is found.

The observed independence of the local derivatives in $\ln x$ at fixed Q^2 suggests that F_2 can be parameterised in a very simple form

$$F_2 = c(Q^2)x^{-\lambda(Q^2)} \ . \tag{3}$$

The results for $\lambda(Q^2)$ are shown in Figure 5 (right). The coefficient $c(Q^2) \approx 0.18$ and the parameterisation $\lambda(Q^2) = a{\cdot}\ln(Q^2/\Lambda^2)$ for $Q^2 \geq 2$ GeV^2 are in accord with pQCD predictions. In contrast, at $Q^2 \leq 1$ GeV^2 the behaviour is changing, and, in the low Q^2 limit, λ is approaching 0.08, which is expected from the energy dependence of soft hadronic interactions $\sigma_{tot} \sim s^{\alpha_P(0)-1} \approx s^{0.08}$.

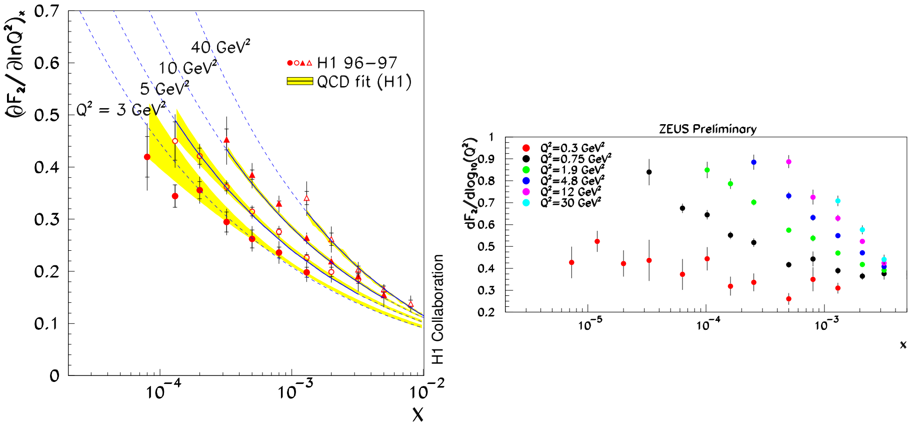

Figure 6. The derivative $(\partial F_2/\partial \ln Q^2)_x$ as function of x for different Q^2.

3.2. *Scaling violations of F_2*

Another important quantity in view of possible non-linear gluon interaction effects is the derivative

$$(\partial F_2(x, Q^2)/\partial \ln Q^2)_x \tag{4}$$

describing scaling violations. Its behaviour in x is a direct reflection of the gluon density dynamics in the associated kinematic range.

The derivatives measured by H1 and ZEUS are shown in Figure 6 as a function of x for different Q^2. They show a continuous growth towards low x down to lowest $Q^2 = 0.3$ GeV^2, without an indication of a change in the dynamics. The derivatives are well described by the pQCD calculations for $Q^2 \geq 3$ GeV^2.

3.3. *Longitudinal structure function $F_L(x, Q^2)$*

Non-zero values of the structure function F_L appear in pQCD due to gluon radiation. Thus, F_L is the most appropriate quantity to test QCD to NLO and especially to examine the pathological effects of the negative gluon distribution discussed in section 2.1.

According to eq. 1, the F_L contribution to the inclusive cross section is significant only at high y. The conventional way to measure F_L is to explore the y dependence of the cross section at given x and Q^2 by changing the center of mass energy of the interaction. Such a measurement is not yet performed at HERA. The H1 collaboration developed other ways to

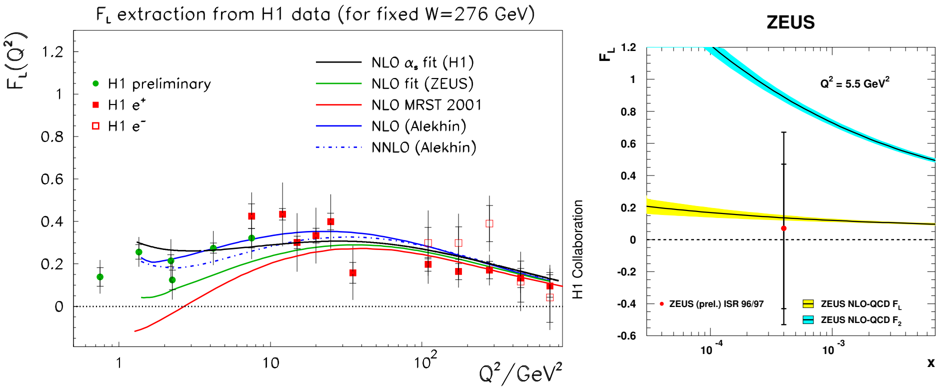

Figure 7. Summary of the F_L measurements by H1 at fixed photon-proton center of mass energy $W = 276$ GeV, $W \approx \sqrt{sy}$ (left). The F_L measurement by ZEUS using radiative events (right).

determine F_L from the measured turn over of the cross section at high y. This becomes possible due to the H1 measurements at very low scattered electron energy down to 3 GeV. The determinations of F_L are based on various methods to propagate F_2 measurements to the region corresponding to high y (low x).

A summary of the F_L measurements by H1 [17] is shown in Figure 7 (left). The results are significantly above zero everywhere, including the lowest Q^2. They are compared with pQCD predictions and different phenomenological models showing that already at the present level of precision the measurements can distinguish different calculations.

The ZEUS collaboration used DIS radiative events with detection of the photon from the initial state radiation (ISR) process in a zero angle photon tagger. ISR effectively reduces the energy of the electron participating in the interaction. The result [18] is shown in Figure 7 (right). Large errors of the measurement suggest that precise direct measurements of F_L at HERA can be performed only by reducing the beam energy and employing the highest y domain.

4. Conclusions

The inclusive DIS cross sections from HERA I cover a kinematic phase space extended towards low x and high Q^2 by two orders of magnitude compared with fixed target experiments. These data, studied in the framework of perturbative QCD in the form of NLO DGLAP analyses, provide an accurate determination of the gluon distribution function. The strong coupling constant $\alpha_s(M_Z^2)$ determined in such analyses has small experimental errors and is currently limited in precision by the accuracy of the NLO theory. No evidence for new QCD effects like saturation has been found in inclusive processes at low x.

The HERA II program, aiming for a 10-fold increase of statistics with a longitudinally polarised electron beam, with much improved H1 and ZEUS detectors, is just starting. A special run with lower proton beam energies is envisaged for direct measurements of F_L at low x.

References

1. Y. L. Dokshitzer, Sov. Phys. JETP **46** (1977) 641;
   V. N. Gribov and L. N. Lipatov, Sov. J. Nucl. Phys. **15** (1972) 438 and 675;
   G. Altarelli and G. Parisi, Nucl. Phys. B **126** (1977) 298.
2. S. Moch, Proc. of Ringberg Workshop "New Trends in HERA Physics 2003".
3. D. Kcira, Proc. of Ringberg Workshop "New Trends in HERA Physics 2003".
4. B. Partheault, Proc. of Ringberg Workshop "New Trends in HERA Physics 2003".
5. H1 Collab., C. Adloff et al., Eur. Phys. J. C **30** (2003) 1.
6. ZEUS Collab., S. Chekanov et al. Phys. Rev. **D67** (2003) 012007.
7. J. Pumplin, D. R. Stump, J. Huston, H. L. Lai, P. Nadolsky and W. K. Tung, JHEP **0207** (2002) 012.
8. A. D. Martin, R. G. Roberts, W. J. Stirling and R. S. Thorne, Eur. Phys. J. C **23** (2002) 73.
9. R. S. Thorne *et al.*, J. Phys. G **28** (2002) 2717.
10. C. Adloff *et al.* [H1 Collaboration], Eur. Phys. J. C **21** (2001) 33.
11. A. D. Martin, R. G. Roberts, W. J. Stirling and R. S. Thorne, Phys. Lett. B **531** (2002) 216.
12. S. I. Alekhin, JHEP **0302** (2003) 015.
13. K. Golec-Biernat and M. Wusthoff, Phys. Rev. D **59** (1999) 014017;
    J. Bartels, K. Golec-Biernat and H. Kowalski, Phys. Rev. D **66** (2002) 014001.
14. E. A. Kuraev, L. N. Lipatov and V. S. Fadin, Sov. Phys. JETP **44** (1976)443;
    E. A. Kuraev, L. N. Lipatov and V. S. Fadin, Sov. Phys. JETP **45** (1977) 199;
    Y. Y. Balitsky and L. N. Lipatov, Sov. Journ. Nucl. Phys. **28** (1978) 822.
15. C. Adloff *et al.* [H1 Collaboration], Phys. Lett. B **520** (2001) 183.
16. H1 Collaboration, contributed paper to EPS03 (2003), Aachen, abstract 082.
17. H1 Collaboration, contributed paper to EPS03 (2003), Aachen, abstract 083.
18. ZEUS Collaboration, contrib. paper to EPS03(2003), Aachen, abstract 502.